World Academy of Science, Engineering and Technology
International Journal of Physical and Mathematical Sciences
Vol:6, No:8, 2012

High Order Accurate Runge Kutta Nodal Discontinuous Galerkin Method for Numerical Solution of Linear Convection Equation

Faheem Ahmed, Fareed Ahmed, Yongheng Guo, Yong Yang

Abstract**—**This paper deals with a high-order accurate Runge Kutta Discontinuous Galerkin (RKDG) method for the numerical solution of the wave equation, which is one of the simple case of a linear hyperbolic partial differential equation. Nodal DG method is used for a finite element space discretization in 'x' by discontinuous approximations. This method combines mainly two key ideas which are based on the finite volume and finite element methods. The physics of wave propagation being accounted for by means of Riemann problems and accuracy is obtained by means of high-order polynomial approximations within the elements. High order accurate Low Storage Explicit Runge Kutta (LSERK) method is used for temporal discretization in 't' that allows the method to be non-linearly stable regardless of its accuracy. The resulting RKDG methods are stable and high-order accurate. The $\mathbf{L_1}$,$\mathbf{L_2}$ and $\mathbf{L_\infty}$ error norm analysis shows that the scheme is highly accurate and effective. Hence, the method is well suited to achieve high order accurate solution for the scalar wave equation and other hyperbolic equations.

Keywords**—**Nodal Discontinuous Galerkin Method, RKDG, Scalar Wave Equation, LSERK

I. Introduction

THE Discontinuous Galerkin (DG) method was first introduced by Reed and Hill [1] as a technique to solve neutron transport problems. Subsequently, the same was analyzed by LeSaint and Raviart [2], Johnson and Pitkar nta [3], Richter [4], and by Peterson [5]. All these were for the linear equations [6]. In a series of papers by Cockburn, Shu et al. [7]-[10], the RKDG method has been developed for solving nonlinear hyperbolic conservation laws and related equations, in which DG is used for spatial discretization with flux values at cell edges computed by either Riemann solvers or monotone flux functions, the Total Variation Bounded (TVB) limiter [10],[11] is employed to eliminate spurious oscillations and the Total Variation Diminishing (TVD) Runge-Kutta (RK) method [12] is used for the temporal discretization to ensure the stability of the numerical approach while simplifying the implementation. The RKDG method has enjoyed great success in solving the Euler equations for gas dynamics, compressible Navier-Stokes equations, viscous magneto hydrodynamic equations and many other equations, and also motivated many related new techniques [13], [18].

All authors are associated with the Northwestern Polytechnical University, Xi'an China. Address: 127 Youyi Xi Lu, Xi'an 710072 Shaanxi. P.R. China. (Corresponding author Mr. Faheem Ahmed Sheikh, Phone: +8618710433933 E-mail: engr_faheem19@hotmail.com & faheemahmed19@yahoo.com).

The DG method has recently become more popular for the solution of systems of conservation laws to arbitrary order of accuracy [14], [18]. An intelligent combination of the Finite Element Method (FEM) and Finite Volume Method (FVM), utilizing a space of basis and test function that mimics the finite element method but satisfying the equation in a sense closer to the finite volume method, appears to offer many of the desired properties. This combination is exactly what leads to Discontinuous Galerkin Finite Element Method (DG-FEM) [15], [18]. The physics of wave propagation is, however, accounted for by solving the Riemann problems that arises from the discontinuous representation of the solution at element interfaces [14], [18].

High order accurate Low-Storage Explicit Runge-Kutta (LSERK) method is used for temporal discretization. Special class of Runge-Kutta time discretization allows the method to be non-linearly stable regardless of its accuracy, with a finite element space discretization by discontinuous approximations that incorporates numerical fluxes and slope limiters coined during the remarkable development of the high resolution finite difference and finite volume schemes. The resulting RKDG methods are stable, high-order accurate and highly parallelizable schemes that can easily handle complicated geometries and boundary conditions [16].

RKDG is applied to linear convection equation as linear and nonlinear convection equations in numerical methods which have wide variety of applications. Referring [17] "Practical problems in which convection plays an important role arise in applications as diverse as meteorology, weather-forecasting, oceanography, gas dynamics, turbo machinery, turbulent flows, granular flows, oil recovery simulation, modeling of shallow waters, transport of contaminant in porous media, visco-elastic flows, semiconductor device simulation, magneto-hydrodynamics, and electro-magnetism, among many others. This is why devising robust, accurate and efficient methods for numerically solving these problems is of considerable importance.''[16]

II. Model Equation

The model hyperbolic equation considered here is linear scalar wave equation and is given as

$$\frac{\partial u}{\partial t} + \frac{\partial f(u)}{\partial x} = 0 \quad , \quad x \in [L, R] = \Omega \tag{1}$$

Where $f(u) = au$

III. Discontinuous Galerkin Formulation

The RKDG method realizes a fortunate compromise between the two numerical schemes i.e. FEM & FVM, by incorporating the ideas of numerical fluxes and slope limiters or filters into a finite element framework. RKDG is applied to the given problem. Stepwise methodology of the same is appended below:

A.DG Spatial Discretization.

First, we discretize (1) in space by using DG approach. Here we consider problem posed on the physical domain Ω with boundary $\partial\Omega$ and assume that this domain is well approximated by the computational domain Ω_h. This is space filling triangulation composed of a collection of K geometry–conforming non-overlapping elements D^k.

Consider the linear scalar wave equation (1), we have

$$\frac{\partial u}{\partial t} + \frac{\partial f(u)}{\partial x} = 0 \quad , \quad x \in [-1,1], \qquad t > 0 \tag{2}$$

Where the flux is given as $f(u) = au \; and \; a > 0$, this is subjected to the appropriate initial and boundary conditions, given as under:

Initial Conditions

$$u(x,0) = u_0(x) = g(x) = sin(\pi x)$$

The solution of the (1) is of the form

$$u(x,t) = u_0(x - at) = sin(\pi (x - at))$$

Boundary conditions

$$u(-1,t) = g(t) = sin(\pi at)$$

We approximate Ω by K non-overlapping elements, $x \in [x_l^k, x_r^k] = D^k$, as illustrated in Fig. 1. On each of these elements we express the local solution as a polynomial of order $N = N_p - 1$

$$u_h^k(x,t) = \sum_{i=1}^{N_p} u_h^k(x_i^k, t) l_i^k(x) = \sum_{i=1}^{N_p} u_{hi}^k(t) l_i^k(x) \tag{3}$$

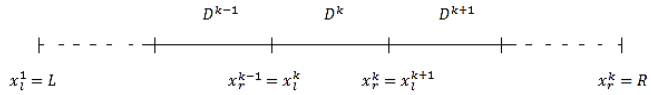

Fig. 1 Computational Domain

In (2) we have applied nodal approach where we introduce $N_p = N + 1$ local grid points, $x_i^k \in D^k$ and express the polynomial through the associated interpolating Lagrange Polynomial $l_i^k(x)$. The global solution is assumed to be approximated by the piecewise N-th order polynomial approximation $u_h(x,t)$, defined as the direct sum of the K local polynomial solution $u_h^k(x,t)$ as in (4).

$$u(x,t) \simeq u_h(x,t) = \bigoplus_{k=1}^{k} u_h^k(x,t) \tag{4}$$

Now we will form the Residual $R_h(x,t)$ of (1)

$$R_h(x,t) = \frac{\partial u_h^k}{\partial t} + \frac{\partial f_h^k}{\partial x} \tag{5}$$

Now we introduce a globally defined space V_h of test functions $\emptyset_h$. Whereas the locally defined space $V_h^k = span\{l_j^k(x)(D^k)\}_{n=1}^{N_p}$. V_h is the space of piecewise smooth functions defined on Ω_h. Locally defined $\emptyset_h \in V_h^k$ of this space and is given as

$$x \in D^k \; : \; \emptyset_h^k(x) = \sum_{n=1}^{N_p} \widehat{\emptyset}_n^k \, l_j^k(x)$$

The residual is to be orthogonal to all the test functions in space V_h and (5) results in the local statement as under

$$\int_{x^k}^{x^{k+1}} R_h(x,t) \, l_j^k(x) dx = 0 \tag{6}$$

The semi discrete weak formulation employs a local discontinuous Galerkin formulation in spatial variables within each element K is written as

$$\int_{D^k} \left(\frac{\partial u_h^k}{\partial t} l_j^k(x) - f_h^k \frac{dl_j^k(x)}{dx} \right) dx + \int_{\partial D^k} \hat{n} \, . \, f^* l_j^k(x) \, dx = 0 \tag{7}$$

Where ∂D^k denotes the boundary of D^k and n̂ representing the local outward pointing normal. In this one-dimensional case, n̂ is simply a scalar and takes value of -1 and +1 at the left and right interface, respectively.

We replace integral using Gauss' theorem to obtain local statement

$$\int_{D^k} \left(\frac{\partial u_h^k}{\partial t} l_j^k(x) - f_h^k \frac{dl_j^k(x)}{dx} \right) dx = -\left[f_h^k l_j^k \right]_{x^k}^{x^{k+1}} \tag{8}$$

The main purpose of the right hand side is to connect the elements. Further, considering the local solution as approximation to the global solution yields the final local semi-discrete scheme as

$$M^k \frac{du_h^k}{dt} - (S^k)^T f_h^k = -\left[f_h^k l_j^k \right]_{x^k}^{x^{k+1}} \tag{9}$$

In (9) M^k and S^k are the mass and stiffness matrices respectively.

Introducing affine mapping

$$x \in D^k : x(r) = \frac{x^k + x^{k+1}}{2} + \frac{x^{k+1} - x^k}{2} r, r \in [-1,1]$$

Length of the element $h^k = x^{k+1} - x^k$

$$M_{ij}^k = \left(l_i^k, l_j^k\right)_{D^k} = \int_{x^k}^{x^{k+1}} l_i^k(x) l_j^k(x) dx \quad (10)$$

$$M_{ij} = \frac{h^k}{2} \int_{-1}^{1} l_i(r)\, l_j(r) dr \quad (11)$$

$$S_{ij}^k = \int_{D^k} l_i^k(x) \frac{dl_j^k}{dx} dx \quad (12)$$

$$S_{ij} = \int_{-1}^{1} l_i(r) \frac{dl_j}{dr}\, dr \quad (13)$$

Similarly right hand side of (9),

$$[l_j^k\ f_h^k]_{x^k}^{x^{k+1}} = [l_j^k \sum_{i=1}^{N_p} f_{hi}^k(t) l_i^k(x)]_{x^k}^{x^{k+1}}$$

Finally, (9) can be written in the matrix form as

$$\frac{h^k}{2}[M]_{n\times n} \frac{d}{dt}\begin{bmatrix} u_{h1}^k \\ u_{h2}^k \\ \vdots \\ u_{hn}^k \end{bmatrix} - [S]_{n\times n}^T \begin{bmatrix} f_{h1}^k \\ f_{h2}^k \\ \vdots \\ f_{hn}^k \end{bmatrix} = f_h^*(x^{k+1}) \begin{bmatrix} 0 \\ 0 \\ \vdots \\ 1 \end{bmatrix} + f_h^*(x^k) \begin{bmatrix} 1 \\ \vdots \\ 0 \\ 0 \end{bmatrix} \quad (14)$$

Lax- Friedrich Flux: Since the numerical solution u_h is discontinuous between element interfaces therefore, we must replace flux f^* by a numerical flux function $f^*(u_L, u_R)$. We have used monotone Lax-Friedrich scheme to calculate the numerical flux

$$f^*(u_L, u_R) = \frac{1}{2}[(f_L + f_R) - C(u_R - u_L)] \quad (15)$$

The constant in the Lax-Friedrich Flux is given as

$$C = max\left|\lambda\left(\hat{n} . \frac{\partial f}{\partial u}\right)\right| \quad (16)$$

Here, the concept of approximate Riemann solver or numerical flux is incorporated into the DG method.

Gram-Schmidt orthogonalization: In order to obtain suitable, accurate and computationally stable solution, orthonormal basis are required. Therefore, we took the monomial basis, r^n, and obtained orthonormal basis through L^2-based Gram-Schmidt orthogonalization approach which results in orthonormal basis. Subsequently, Vandermode matrix was formed by using normalized polynomials and the same was then used to compute Mass and Stiffness matrices.

B.LSERK Temporal Discretization

Subsequent to space discretization, the resulting system of Ordinary Differential Equations (ODE) can be written in the form as:

$$M \frac{du_h}{dt} = R(u_h, t) \quad (17)$$

Where M denotes the mass matrix, u_h is the global vector of n degrees of freedom, and $R(u_h, t)$ is the residual vector. By using the following high-order accurate Low-Storage Explicit Runge–Kutta (LSERK) method, (17) is further discretized:

1) Set $p^{(0)} = u^n$,

2) Compute the intermediate functions:

$$i \in [1, \ldots, 5] : \begin{cases} k^{(i)} = \alpha_i k^{(i-1)} + \Delta t\, L_h\left(p^{(i-1)}, t^n + \gamma_i \Delta t\right) \\ p^{(i)} = p^{(i-1)} + \beta_i k^{(i)} \end{cases},$$

3) Set $u_h^{i+1} = p^{(5)}$

TABLE I
COEFFICIENTS FOR THE LOW STORAGE FIVE STAGE FOURTH ORDER EXPLICIT RUNGE-KUTTA METHOD

i	α_i	β_i	γ_i
1	0.0000000000	0.1496590220	0.0000000000
2	-0.4178904745	0.3792103130	0.1496590220
3	-1.1921516950	0.8229550294	0.3704009574
4	-1.6977846920	0.6994504559	0.6222557631
5	-1.5141834440	0.1530572480	0.9582821307

IV. NUMERICAL RESULTS

The results obtained are depicted in the following figures:

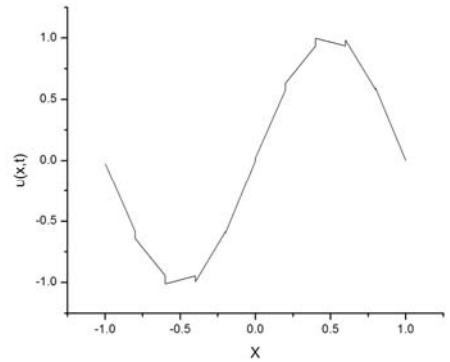

Fig. 2 Numerical Solution at N=1,K=10 and T =10

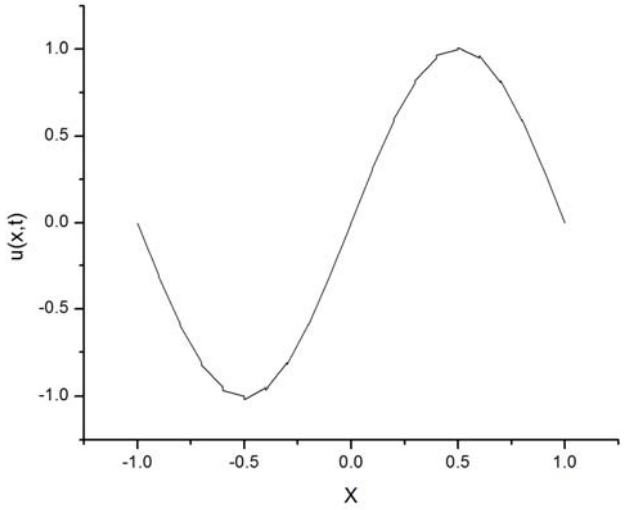

Fig. 3 Numerical Solution at N=1, K=20 and T =10

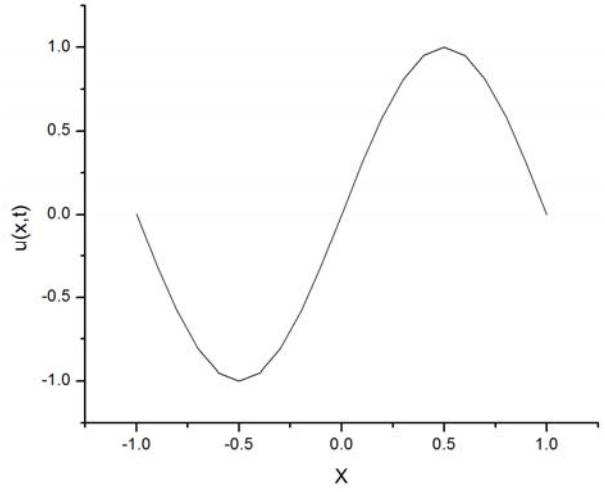

Fig. 4 Numerical Solution at N=2, K=10 and T =10

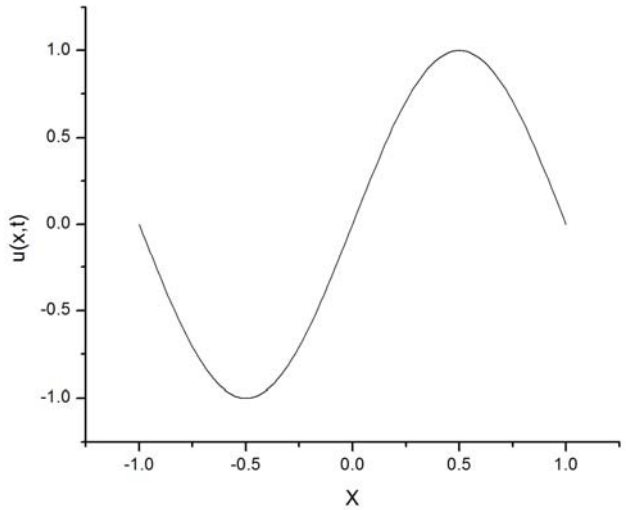

Fig. 5 Numerical Solution at N=4, K=30 and T =10

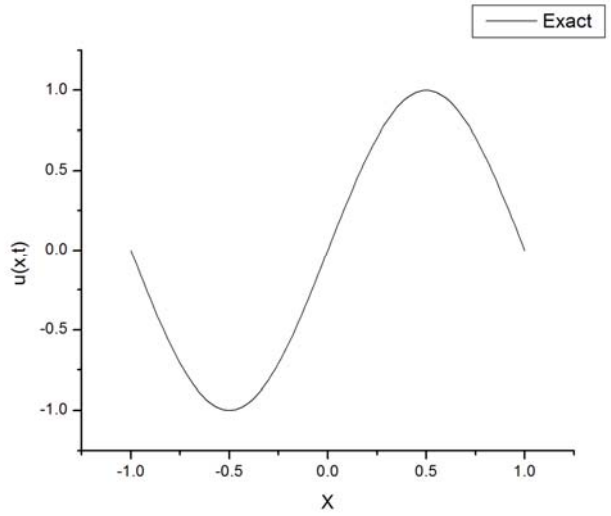

Fig. 6 Exact Solution at N=4, K=30 and T =10

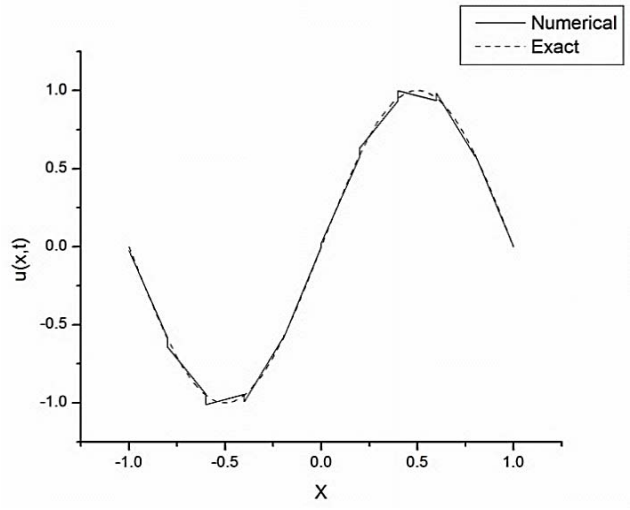

Fig. 7 Numerical Solution at N=1, K=10 and T=10

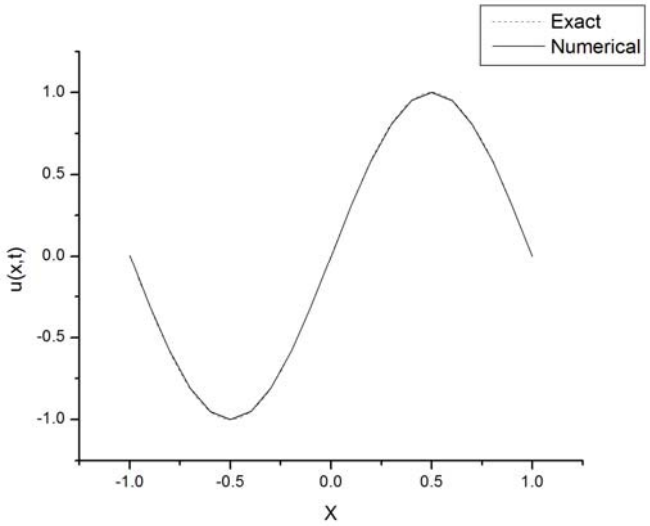

Fig. 8 Numerical Solution at N=2, K=10 and T=10

V. Error Estimations

Following error norms are used to measure the accuracy:

1) $\mathbf{L_1}$ – error

$$\|e\|_{L_1} = \sum_{i=1}^{n} |e_i|$$

2) $\mathbf{L_2}$ – error

$$\|e\|_{L_2} = \left(\sum_{i=1}^{n} |e_i|^2 \right)^{\frac{1}{2}}$$

3) $\mathbf{L_\infty}$ – error

$$\|e\|_{L_\infty} = max|e_i| \ , 1 \le i \le n$$

TABLE II
L_1, L_2 AND L_∞ ERROR NORMS WITH VARIABLE STEP SIZES, POLYNOMIAL ORDER (P) AND OBSERVED ORDER OF ACCURACY (O)

p^1						
Step Size	L_1	***O***	L_2	***O***	L_∞	***O***
h	4.14E-01	------	1.26E-01	------	5.95E-02	------
2/3(h)	2.77E-01	0.98	7.19E-02	1.38	2.77E-02	1.89
1/2(h)	2.09E-01	0.98	4.79E-02	1.41	1.57E-02	1.96
2/5(h)	1.67E-01	0.99	3.49E-02	1.43	1.01E-02	1.98
1/3(h)	1.39E-01	0.99	2.68E-02	1.44	7.10E-03	1.94
p^2						
Step Size	L_1	***O***	L_2	***O***	L_∞	***O***
h	3.25E-02	------	9.40E-03	------	3.94E-03	------
2/3(h)	1.46E-02	1.97	3.44E-03	2.48	1.22E-03	2.90
1/2(h)	8.25E-03	1.99	1.68E-03	2.49	5.11E-04	3.02
2/5(h)	5.27E-03	2.01	9.62E-04	2.49	2.64E-04	2.96
1/3(h)	3.65E-03	2.01	6.10E-04	2.50	1.52E-04	3.01
p^3						
Step Size	L_1	***O***	L_2	***O***	L_∞	***O***
h	1.68E-03	------	4.29E-04	------	1.84E-04	------
2/3(h)	4.91E-04	3.03	1.04E-04	3.49	3.64E-05	3.99
1/2(h)	2.08E-04	2.98	3.81E-05	3.50	1.15E-05	4.02
2/5(h)	1.06E-04	3.01	1.75E-05	3.50	4.74E-06	3.96
1/3(h)	6.16E-05	2.99	9.23E-06	3.50	2.29E-06	3.99
p^4						
Step Size	L_1	***O***	L_2	***O***	L_∞	***O***
h	5.95E-05	------	1.50E-05	------	6.19E-06	------
2/3(h)	1.20E-05	3.94	2.42E-06	4.49	8.50E-07	4.90
1/2(h)	3.82E-06	3.99	6.64E-07	4.50	2.00E-07	5.03
2/5(h)	1.56E-06	4.01	2.43E-07	4.51	6.61E-08	4.96
1/3(h)	7.53E-07	4.00	1.06E-07	4.52	2.63E-08	5.04

VI. Error Norm Analysis

Following figures give the overall analysis of the numerical solution that varies by varying the step size and changing the polynomial order:

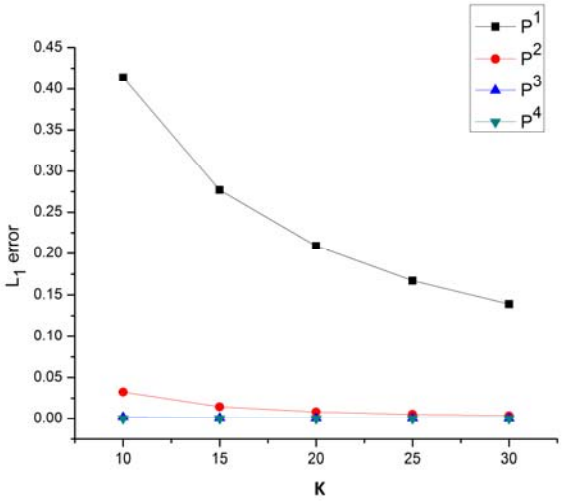

Fig. 9 $\mathbf{L_1}$ error norm with different K and N

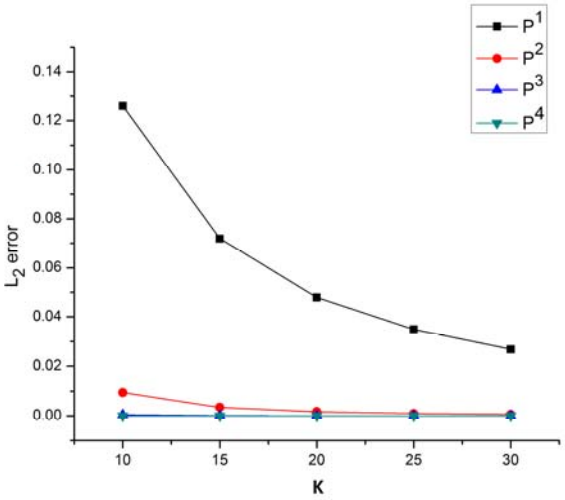

Fig. 10 $\mathbf{L_2}$ error norm with different K and N

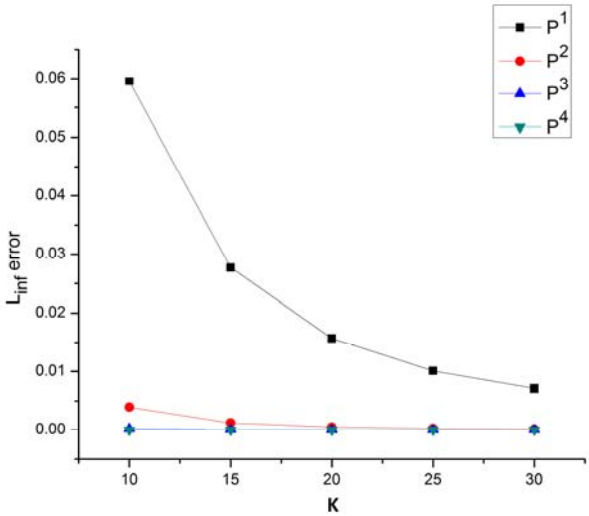

Fig. 11 $\mathbf{L_\infty}$ error norm with different K and N

VII. Conclusion

The numerical solution of the linear convection equation, obtained by using RKDG is highly accurate and nearly the same as exact solution as shown in Fig. 7. Moreover, Figs. 2, 3, 4 & 5 clearly depicts that the accuracy of the numerical solution is increasing by decreasing the step size (*h*) and increasing order of polynomial. Results reveal that the accuracy of the solution is increased by:

1) Reducing the step size at fix order of polynomial
2) Increasing the order of polynomial at fix step size
3) Varying the both step size and order of polynomial that is by reducing the step size and increasing the order of polynomial.

In order to obtain the observed order of accuracy (O), $\mathbf{L_1}$,$\mathbf{L_2}$ and $\mathbf{L_\infty}$ error norm analysis is also performed and tabulated in Table-II. After evaluating the numerical results, it is found that RKDG method with *hp* combination is highly accurate and stable and hence well suited to obtain solution of convection/advection problems.

References

[1] W.H. Reed and T. Hill. Triangular mesh methods for the neutron transport equation. Tech. report LA-UR-73-479, Los Alamos Scientific Laboratory, 1973.
[2] P. LeSaint and P. A. Raviart, On a finite element method for solving the neutron transport equation, Mathematical aspects of finite elements in partial differential equations (C. de Boor, Ed.), Academic Press, 89 (1974).
[3] C. Johnson and J. Pitkäranta, An analysis of the discontinuous Galerkin method for a scalar hyperbolic equation, Math. Comp. 46, 1 (1986).
[4] G. R. Richter, An optimal-order error estimate for the discontinuous Galerkin method, Math. Comp. 50, 75(1988).
[5] T. Peterson, A note on the convergence of the discontinuous Galerkin method for a scalar hyperbolic equation, SIAM J. Numerical. Analysis. 28, 133 (1991).
[6] B. Cockburn and C. W. Shu, "The Runge-Kutta Discontinuous Galerkin Method for conservation laws V: Multidimensional System," Journal of Computational Physics, Vol. 141, pp. 199-224, 1998.
[7] B. Cockburn and C.-W. Shu. The TVB Runge-Kutta local projection discontinuous Galerkin finite element method for conservation laws V: multidimensional systems. J. Comput. Phys., 141:199–224, 1998.
[8] B. Cockburn, S. Hou and C.-W. Shu. The TVB Runge-Kutta local projection discontinuous Galerkin finite element method for conservation laws IV: the multidimensional case. Math. Comp., 54:545–581, 1990.
[9] B. Cockburn, S.-Y. Lin and C.-W. Shu. TVB Runge-Kutta local projection discontinuous Galerkin finite element method for conservation laws III: one dimensional systems. J. Comput. Phys., 52:411–435, 1989.
[10] B. Cockburn and C.-W. Shu. TVB Runge-Kutta local projection discontinuous Galerkin finite element method for conservation laws II: general framework. Math. Comp., 52:411– 435, 1989.
[11] C.-W. Shu. TVB uniformly high-order schemes for conservation laws. Math. Comp.,49:105–121, 1987.
[12] C.-W. Shu and S. Osher. Efficient Implementation of essentially non-oscillatory shock capturing schemes. J. Comput. Phys., 77:439–471, 1988.
[13] ZhiliangXu, Yingjie Liu "A Conservation Constrained Runge-Kutta Discontinuous Galerkin Method with the Improved CFL Condition for Conservation Laws" February 16, 2010.
[14] H. Luo, J. D. Baum, and R. Lohner, "A Hermite WENO-based Limiter for Discontinuous Galerkin Method on Unstructured Grids", 45th AIAA Aerospace Sciences Meeting and Exhibit, 8–11, January 2007, Reno, Nevada
[15] Jan S. Hesthaven Tim Warburton "Nodal Discontinuous Galerkin Methods"- Algorithms, Analysis, and Applications" (2008).
[16] B. Cockburn and C.WShu "Runge–Kutta Discontinuous Galerkin Methods for Convection-Dominated Problems" Journal of Scientific Computing, Vol. 16, No. 3, September 2001 (2001).
[17] B. Cockburn, G.E. Karniadakis and C.-W. Shu. (2000).The development of discontinuous Galerkin methods. In B. Cockburn, G.E. Karniadakis and C.-W. Shu (eds), Discontinuous Galerkin Methods. Theory, Computation and Application, Lecture Notes in Computational Science and Engineering, Vol. 11, Springer-Verlag, pp. 3-50.
[18] Fareed Ahmed, Faheem Ahmed, Yongheng Guo, andYong Yang, "A High Order Accurate Nodal Discontinuous Galerkin Method (DGM) for Numerical Solution of Hyperbolic Equation," International Journal of Applied Physics and Mathematics vol. 2, no. 5, pp. 362-364, 2012.